Pertanika J. Sci. & Technol. 27 (4): 2439 - 2452 (2019)

PERTANIKA JOURNALS

SCIENCE & TECHNOLOGY

Journal homepage: http://www.pertanika.upm.edu.my/

Scattered Radiation Dose Calculation in the Multi-Bay Resuscitation Room using MCNP5 Code

Marianie Musarudin[1]*, Ruzainah Mohd Nordin[1] and Nik Kamarullah Ya Ali[2]

[1]*School of Health Sciences, Health Campus, Universiti Sains Malaysia, 16150 USM, Kubang Kerian, Kelantan, Malaysia*

[2]*Department of Radiology, Hospital Universiti Sains Malaysia, 16150 USM, Kubang Kerian, Kelantan, Malaysia*

ABSTRACT

This study aims to characterise the scattered dose distribution from a ceiling-mounted X-ray unit in a multi-bay resuscitation room. The finding of this study is essential for optimisation and safety of staff and patients. Simulation of phantom imaging was carried out using MCNP5 code. The calculated data were initially compared against the measurements carried out using a survey meter. Three measurement positions, denoted by T2, T3, and T4 were considered for the dose calculation. The data suggested that T2 received the highest scattered dose. This value (maximum value of less than 6 μGy) is lower than the annual dose limit for the public and radiation workers as well as natural background radiation dose. Meanwhile, T3 consistently received a higher scattered dose (maximum difference of 25.62%) than T4. The angles of the X-ray tube resulted in scattered doses less than 6 μGy for both 90^o and 100^o scattering angles. In conclusion, the scattered dose for a single exposure imaging inside the room is safe. Yet, consideration of the placement of a portable lead shielding between X-ray tube and treatment couch is strongly recommended. This is due to a high number of imaging procedures commonly performed daily in a busy hospital. Hence, the cumulative dose to the paramedic staff and patients may exceed the safe level.

Key-words: MCNP5, scattered dose, x-ray room

ARTICLE INFO

Article history:
Received: 13 May 2019
Accepted: 03 July 2019
Published: 21 October 2019

E-mail addresses:
marianie@usm.my (Marianie Musarudin)
eina8_nordin@yahoo.com.my (Ruzainah Mohd Nordin)
kamarullah@usm.my (Nik Kamarullah Ya Ali)
* Corresponding author

INTRODUCTION

The guidelines for a safe level of exposure to radiation for medical purposes for staff and patient have been tightened by the International Commission on Radiological Protection (ICRP). This enforcement is due to the increase in the use of radiation for

ISSN: 0128-7680
e-ISSN: 2231-8526

medical purposes. In comparison to the early 1980s, the exposure to ionizing radiation from medical diagnostics has increased up to seven times. According to Report No. 160 released by the National Committee on Radiological Protection (NCRP) in 2009, the collective effective dose for X-ray examinations represented 5% of all exposure categories (David & Otha, 2009).

Measurement of the doses for an X-ray room is commonly performed at several points outside the planned location for a shielding barrier. For instance, doses at the walls and doors are commonly assessed as a part of radiation protection monitoring. This is an important practice to determine the amount of scattering inside and outside the radiation room. The primary, scatter, and leakage radiations are necessary factors to be considered during the design phase of the X-ray room. Therefore, previous studies had commonly presented the transmission data for various materials of the shield used in X-ray room such as lead, concrete, gypsum wallboard, steel, and plate glass (Archer et al., 1994; Simpkin, 1989; Simpkin, 1995). The difference between the penetrating powers of the X-ray produced by single and three-phase generators has also been highlighted in these studies. In other studies, the main focus was on the amount of dose absorbed by staff at several positions around patient being exposed to the ionizing radiation. Previously, the scattered dose absorbed by an infant being administered a chest radiograph was shown to be less than the background radiation (Catherine et al., 2009; Trinh et al., 2010). Similar findings were concluded for the assessment of the scattered dose absorbed by technicians at different distances from X-ray exposure (Chiang et al., 2015).

Nevertheless, the research interest of this study is not on the effectiveness of shielding material in an X-ray room. Rather, the distribution of scattered dose inside the X-ray room is the focus of this study. An X-ray room is known to be commonly equipped with a single X-ray unit. Therefore, the dose distribution inside an X-ray room was not much of a concern previously. Meanwhile, our X-ray room is equipped with a newly-designed Direct Digital Radiography (DDR) system, a Samsung Varian Transbay DDR X-ray machine, model GC85A. This system is equipped with a railing system that moves the X-ray tube 6504 mm in the y-direction and 4010 mm in the x-direction. In accordance with that, the patient exposure can generally be performed at two different bed positions. Even though the single X-ray tube allows a single exposure at a time, simultaneous preparation of another patient for the next exposure will improve the patient throughput and consequently reduce the waiting time. In addition, this imaging room is equipped with two patient couches at a distance of 4000 mm from the X-ray tube position. Accordingly, consideration of the unplanned amount of scattered dose absorbed by patient due to X-ray exposure inside the room is necessary for his/her safety. This is in line with the guidelines set by ICRP on the safe levels of exposure to medical radiation for staff and patients. Therefore, the amount of unnecessary exposure to the patients and the staff should be well observed.

In this study, Monte Carlo modelling of the scattered dose distribution in the multi-bay resuscitation room is performed using MCNP5 code. Wide application of Monte Carlo in medical physics was previously published, which includes dose assessment for many applications related to medical physics (Chiang et al., 2015; Lawrence et al., 2015; McVey & Weatherburn, 2004)**.** The scattered dose from a solid phantom of tissue substitute was calculated as a representative of the scattering behaviour in a patient's body. The calculated data were initially verified against the measurements carried out in the room. The simulation provided new data by calculating the scatter dose distribution inside the imaging room for varying imaging conditions. Nevertheless, the method described in this work is generally applicable for any imaging room.

METHODS

The scattered radiation dose absorbed by patient or staff during a single X-ray examination was calculated inside the multi-bay resuscitation room. Figure 1 shows the schematic illustration of the experimental setup utilising a general-purpose Monte Carlo code version MCNP5. The modelling was designed to be as precise as the real multi-bay resuscitation room in our institution. This precision is necessary to reproduce the same radiation interaction inside the imaging room. This study had modelled 10765 mm x 7868 mm room dimension, patient couches, X-ray beam, and concrete wall. Four patient couches positioned inside the room were modelled via 6 mm thick of water material (Goertz et al., 2015). The distances between the couches were 2990 mm (between T1 and T2) and 3120 mm (between T3 and T4) in the y-direction. Meanwhile, the x-direction distance between the couches were 4000 mm.

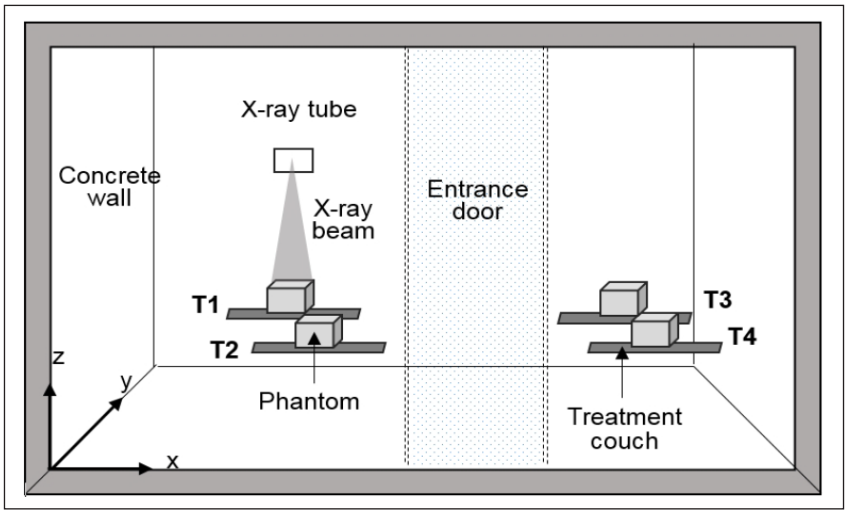

Figure 1. Illustration of the multi-bay resuscitation room modelled using MCNP5 code. T1 and T2 are the couches for X-ray beam exposure, while T3 and T4 are the treatment couches for patients

Three measurement positions were considered during the calculation, labelled as T2, T3, and T4. These positions were selected due to the higher probability that a staff or a patient will be present at the respective positions during imaging. A 30 x 30 x 30 cm solid phantom of tissue substitute was positioned on the patient couch labelled T1, at a source-to-surface distance (SSD) of 100 cm from the X-ray tube focus. An X-ray beam was vertically projected on the upper surface of the phantom. The calculated data were then used to deduce the scattering radiation for the respective clinical settings. The height of the detector was fixed at 90 cm above the floor, which was at the same level of a patient lying on the couch. Hence, measurements were obtained at a scattering angle of 90° with a tube voltage of 125 kV for an incident field area of 900 cm^2. Figure 2 illustrates the experimental setup. The 125 kV energy spectrum was adapted from the Siemens online tool for the simulation of X-ray spectra. The spectrum was collimated into a cone of direction, projected onto the surface of the solid phantom of tissue substitute, modelled to simulate a patient X-ray imaging.

Initially, the calculated data were verified against the measured data obtained using Fluke 481 Radiation Survey meter (David & Otha, 2009; Owusu-Banahene et al., 2018). This step was performed to validate the accuracy of our model as well as the scattered dose estimation. This precision is necessary in order to perform a simulation with similar characteristics as the real room condition. Hence, accurate estimation of the scattering activities in the room could be produced. For each measurement position, the exposure rate at the periphery of the couch was recorded. The survey meter was held at 90 cm height from the floor, to measure the exposure rate at the same level of a patient lying on the couch. The average measured exposure rate was then considered for scattered dose calculation.

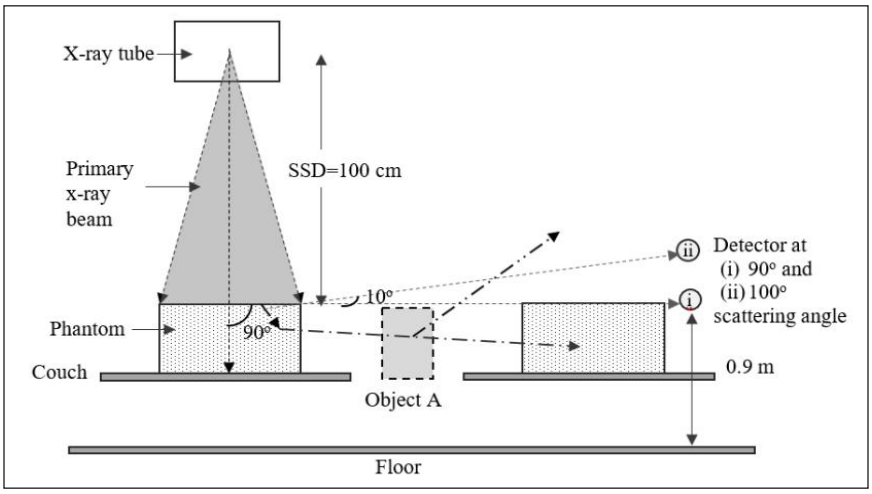

Figure 2. The experimental setup for exposure rate measurement and simulation from a solid phantom of tissue substitute exposed to the X-ray beam. Object A represents the other equipment present in the X-ray room that may lead to other scatter interactions

The mean value of the measured exposure rate was converted to the absorbed dose inside a water phantom. Given, the average energy dissipated in the production of a single ion pair in the air is 34 eV, 1 eV equals to 1.6 x 10^{-19} J, and the charge on a single ion is 1.6 x 10^{-19} C. Therefore, the absorbed dose (in a unit of Gy) is presented by Equation 1, whereby X refers to the exposure in the unit of mR, μ is the mass attenuation coefficient, and 2.58 x 10^{-7} is the mR to C kg^{-1} conversion coefficient (Thomas & Herman, 2009).

$$D_{Exp} = X \times (2.58 \times 10^{-7}) \times 34 \times \left(\frac{\mu_{water}}{\mu_{air}}\right)_{mass} \qquad (1)$$

Meanwhile, the dose or energy deposition in the target cell was scored using *F8 and F6 tally in MCNP5 calculation. The *F8 tally gives an average energy deposited in a unit of MeV. The average energy (E) was then converted to absorbed dose by using Equation 2, whereby 1.602 x 10^{-10} is the MeV g^{-1} to Gy conversion factor. The mass (m) of the cell was determined by multiplying the density of material in the cell and the volume of the cell. In addition to that, the total dose in a water phantom was calculated with the consideration of the X-ray tube efficiency, the tube current, and the exposure time. The X-ray tube efficiency for the 125 kVp tube voltage is equal to 0.01 (Hertrich, 2005).

$$D_{MCNP5} = \left[\frac{E}{m} \times (1.602 \times 10^{-10})\right] \qquad (2)$$

The F6 tally, which gives data in the unit of MeV/g was converted to the absorbed dose by multiplying with 1.602 x 10^{-10} Gy. Similar consideration of the X-ray tube efficiency, tube current, and exposure time were also calculated. The simulation was performed using 10^6 particles to achieve small relative errors (less than 0.10) and pass the statistical checks performed by the package. The relative error less than 0.10 shows a reliable confidence interval and eventually is a measure of the computational precision. Each of the simulations was then repeated using three different seed numbers to observe the reproducibility of the data. The error (E_r) between the simulated (D_{MCNP5}) and the measured (D_{Exp}) values was calculated through the percentage of deviation between the two values, as described by Equation 3 (Gu´erin & Fakhri, 2008).

$$E_r = \frac{|D_{MCNP5} - D_{Exp}|}{D_{Exp}} \times 100 \qquad (3)$$

In this study, we have considered several imaging conditions to be assessed such as the phantom size, the beam collimation size, and the beam projection angles. Figure 3 shows the illustration of the nine beam projection angles modelled using the Monte Carlo code. For the subsequent experiments, the calculations were performed at scattering angles of 90^o and 100^o. The 90^o scattering angle represented the patient lying on the couch, while the

100° scattering angle represented the scattered dose absorbed by patient or staff standing at their respective positions. Figure 2 illustrates the two scattering angles.

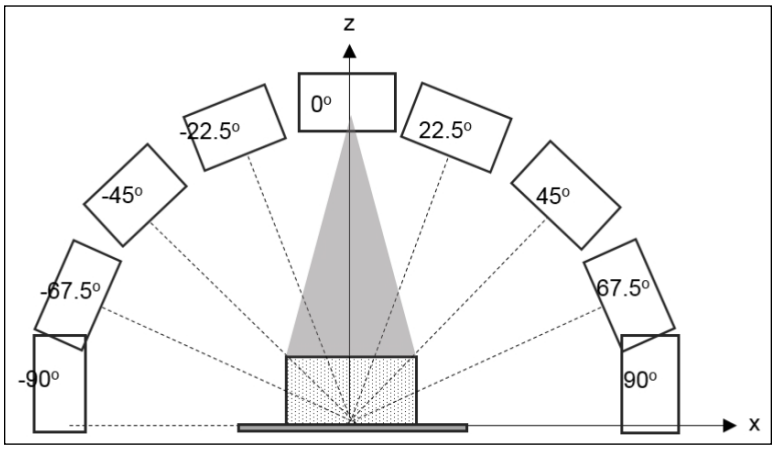

Figure 3. Assuming that the vertical projection was 0° projection, the source of the beam was angled at 22.5° step each

In this study, the MCNP5 code was defined to transport the X-ray beam to the phantom volume, which was modelled to represent the patient's body. Therefore, the estimation of the scattered dose that would be absorbed by patient or staff was calculated by the amount of dose absorbed by the solid phantom of tissue substitute. In addition to the photon and phantom interaction that leads to the initiation of the Compton scattering interaction, the presence of other materials inside the room enhances the scatter interaction

Table 1
The density and composition of the materials defined in the MCNP5 code

		Material			
		Air	Water	Concrete	Lead
Density (g cm^{-3})		0.001205	1.00	2.30	11.35
Elemental composition (%)	H	-	11.19	1.00	-
	C	0.01	-	0.10	-
	N	75.53	-	-	-
	O	23.18	88.81	52.91	-
	Na	-	-	1.60	-
	Mg	-	-	0.20	-
	Al	-	-	3.39	-
	Si	-	-	33.70	-
	K	-	-	1.30	-
	Ca	-	-	4.40	-
	Fe	-	-	1.40	-
	Ar	1.28	-	-	-
	Pb	-	-	-	100.00

(McVey & Weatherburn, 2004). In our code, only the main equipment necessary for the assessment were considered. Therefore, the difference between the MCNP5 scattered dose and the measured scattered dose was expected. Table 1 tabulates the density and the material composition used in the MCNP5 calculation. The density and the composition of materials used in this simulation were obtained from the National Institute of Standards and Technology (NIST).

RESULTS AND DISCUSSION

The scattered doses calculated from the measured exposure rate are tabulated in Table 2. The scattered doses measured at T3 and T4 were much lower than those measured at T2. Higher scattered dose obtained at T2 was expected, due to the positioning of the X-ray tube which was nearer to the T2 position. According to the inverse square law, the radiation intensity is inversely proportional to the square of the distance from the source. Hence, as T2 was nearer to the X-ray tube, it led the positioned phantom to absorb more radiation and doses compared to T3 and T4. Nevertheless, the value was still lower than the annual dose limit for the public and radiation workers as recommended by the Basic Safety Standard regulations. In addition, this value was lower than the natural background radiation dose (8.493 μGy per day) (Trinh et al., 2010).

Table 2
The absorbed dose calculated from the measured exposure rate at four measurement points around the couch (SD=standard deviation)

	Absorbed dose (μGy)		
	T2	T3	T4
Point 1	5.24	2.81	4.07
Point 2	1.36	2.81	0.87
Point 3	6.21	3.01	2.52
Point 4	9.89	2.81	2.33
Mean	5.68	2.86	2.45
SD	3.51	0.10	1.31

Figure 4 shows the comparison between the scattered doses calculated using *F8 and F6 tally. A small error of 2.22% was observed between the two. Accordingly, subsequent experiments to calculate the scattered doses were performed using *F8 tally only. On the other hand, the data compared between measurements and MCNP5 simulation showed significant difference. Maximum difference of 31.8% was calculated between the two. The overestimation of the MCNP5 absorbed dose was most probably due to the simplicity of the room modelled in MCNP5 code. Although the real room is furnished with equipment such as trolley, chairs, and accessories, our MCNP5 code only considered the main equipment

and modality necessary for the assessment. Figure 2 shows the schematic diagram of the interaction between the scattered photon and object A (represents other equipment present inside the room). This illustration is intended to describe the effect of simple geometry modelled in MCNP5 simulation as compared to the actual environment in the X-ray room. Without the object A, the scattered photon may directly hit the phantom next to the phantom exposed to the X-ray beam (shown by dash-dot line). However, with the presence of object A, the photon may scatter and deviate from its trajectory (shown by dash-dot-dot line) and eventually miss the next phantom. Nevertheless, similar trends of dose distribution were observed between the two methods of measurement.

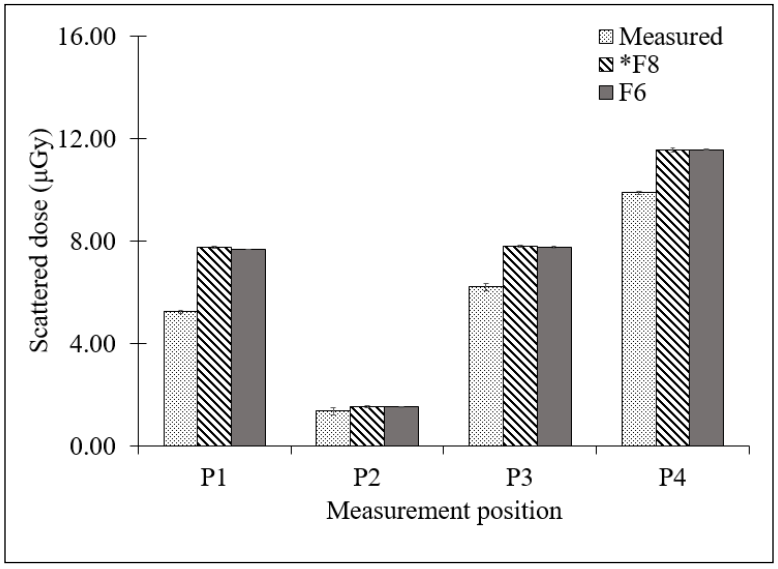

Figure 4. Comparison of the measured and MCNP5 calculated scattered dose. Error bar represents the standard deviation of the data

Although the measurement of exposure rate yielded a low amount of scattered dose inside the imaging room, scattered dose resulted from other exposure settings should be confirmed as well. With respect to that, the MCNP5 simulation was extended to provide calculated scattered dose for other imaging conditions. Figure 5 shows the increment of the scattered dose in correlation with the increment of the phantom size. This increment is expected, considering that the patient's body is known to be the main source of scattering interaction in medical imaging. Referring to the photon interaction cross-section, the probability of Compton interaction is high for the energy range involved in diagnostic radiology imaging. This probability increases as the patient's body size increases, due to the dependency of the Compton interaction on the electron per unit volume (product of physical and electron density). A scattered dose of approximately 21 μGy was calculated at T2 position when a 40 x 40 x 40 cm phantom was exposed to the beam. Indeed, the value

was approximately three times higher than the daily background radiation dose. For that reason, greater safety precaution should be considered when imaging larger-sized patients as the body could be a source of intense scatter interaction. On the other hand, calculations revealed that T3 and T4 positions still received lesser amount of scattered dose than the daily background radiation dose, even for the biggest phantom tested.

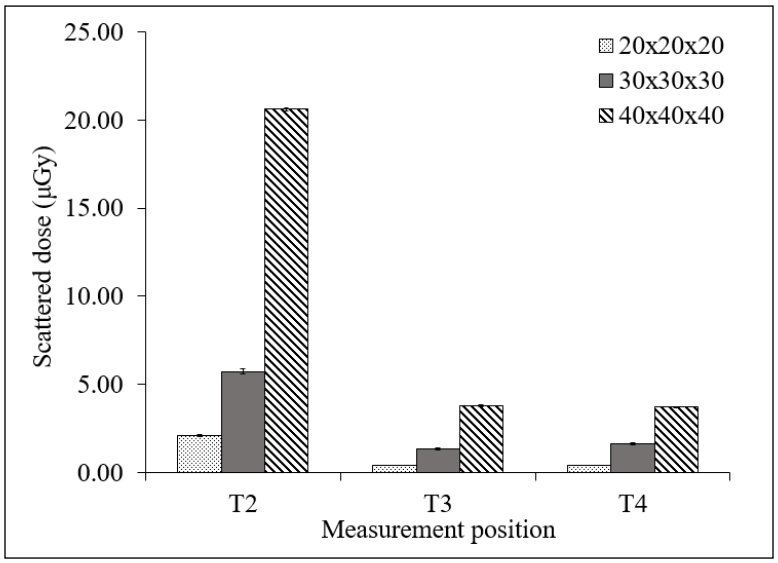

Figure 5. MCNP5 calculated absorbed dose for the different sizes of the phantom. Error bar represents the standard deviation of the data

The comparison shows that the scattered doses calculated at T3 and T4 positions were up to 82% less than the amount calculated at T2 position. In addition, the comparison shows that the scattered doses calculated at T3 and T4 were not significantly varied in the three phantom sizes tested. Nevertheless, the scatter value calculated at T3 was observed to be slightly higher than that calculated at T4. The maximum difference of approximately 16.35% was observed between the two Transbay positions. A similar trend was also observed for the different sizes of beam collimation (Figure 6). Again, T3 recorded higher scattered dose as compared to T4. The maximum difference of 25.62% was recorded between the two. For the 30 x 30 cm beam collimation, greater attention should be given to the T2 position considering that a single exposure could result in a scattered dose that exceeds the daily background radiation.

Calculation of the scattered dose was then extended to the different angles of the X-ray tube. The source angled at 90^{o} in the x and y-directions was considered to evaluate the scattered dose to the three bed positions. These angles were considered to simulate the different beam projections that could be performed during imaging. Figure 7 shows the variation of the scattered dose absorbed by a patient at a 90^{o} scattering angle for the

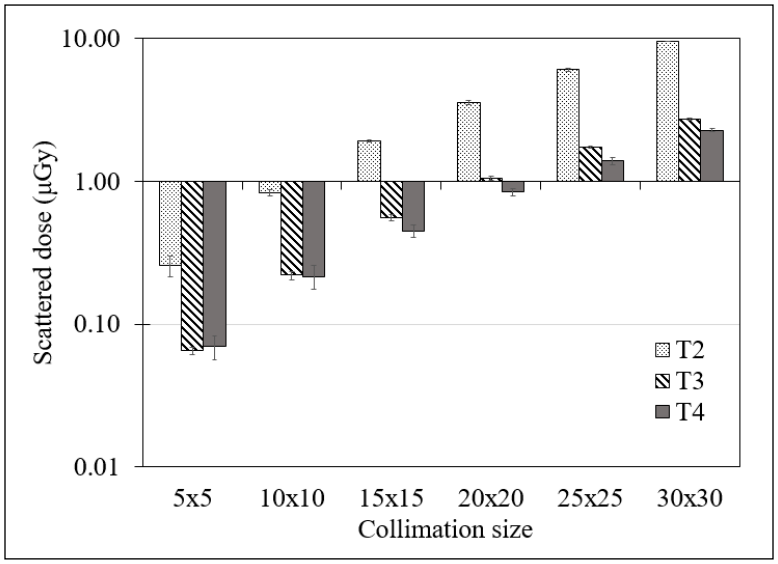

Figure 6. MCNP5 calculated scattered dose for the beam collimation in the range of 5x5 to 30x30. Error bar represents the standard deviation of the data

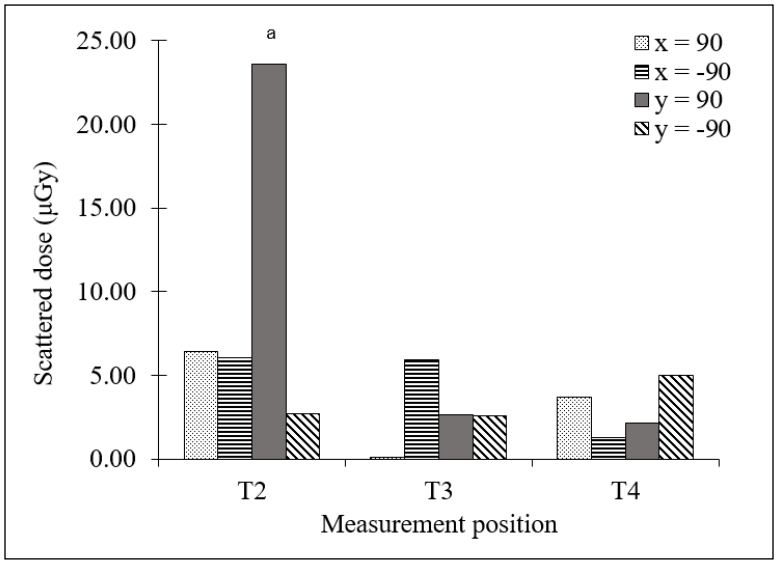

Figure 7. The scattered dose obtained from a collimated cone source angled at 90° in the x and y-directions

investigated angles. The result shows that a relatively low scattered dose was measured at the three positions. The maximum scattered dose of approximately 6 μGy was measured for the tested angles. Nevertheless, the projection parallel to T2 position could result in significant amount of scattered dose to the patient unplanned for exposure at T2 position (denoted by [a] in Figure 7). However, it should be noted that this projection has never been

implemented in our institution. In conclusion, the amount of scattered dose measured for the commonly practiced exposure angles tested is safe and even lower than the annual dose limit for the public and radiation workers. The value is also lower than the natural background radiation dose. To evaluate the scattered doses deposited within the phantom's volume at two patient positioning, 90° and 100° scattering angles were assessed. As shown in Figure 8(a) to Figure 8(c), higher amount of scattered doses were calculated when the projection

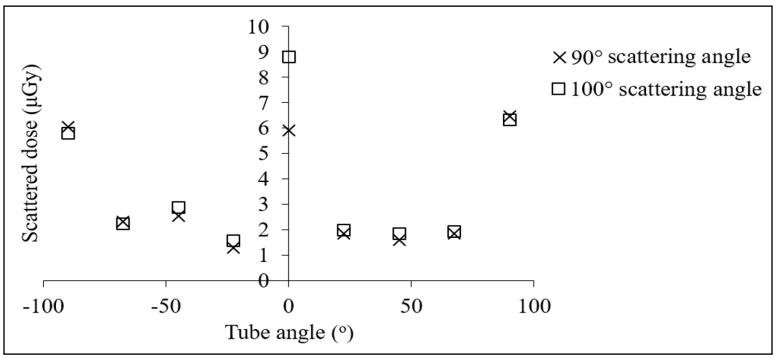

(a)

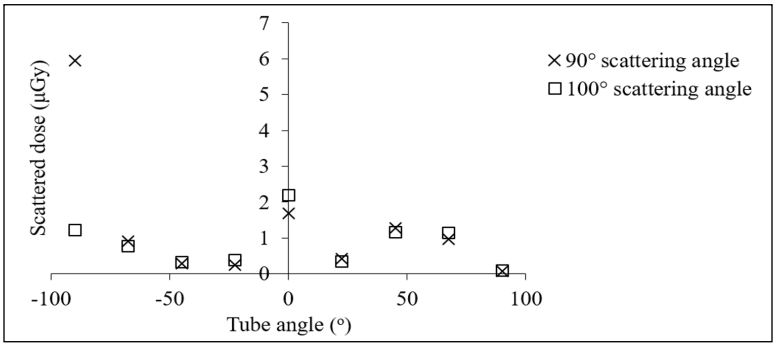

(b)

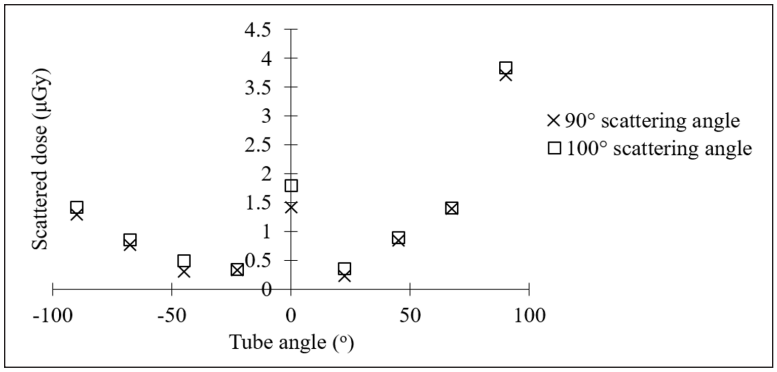

(c)

Figure 8. The scattered dose calculated for the range of 0° to 180° tube angles in the x-direction, while the measurements were calculated at 90° and 100° scattering angles at (a) T2 (b) T3 and (c) T4

was made at 0^o and 90^o (both positive and negative directions) tube angles. The maximum difference of 48.65% was calculated between the two. Meanwhile, a small difference was observed between the two scattering angles for the tube angles of 22.5^o to 67.5^o (in either positive or negative direction). The high value of the scattered dose was calculated at T3 when the exposure was performed at -90^o tube angle due to the direct projection of the beam towards the T3 position. However, this projection is also never being practiced in our institution. Therefore, the data showed that the amounts of the scattered doses were within safe level for all angles assessed. For the 100^o scattering angle, the amount of scattered dose at T2 may slightly exceed the daily background radiation dose when the exposure was performed at 0^o tube angle.

With the concern that T2 had consistently received the highest scattered dose compared to T3 and T4 positions, a lead shielding was proposed to be positioned between the two to reduce such exposure. The portable lead shield with the distance range of 20 cm to 100 cm to the X-ray tube position was modelled using MCNP5 code. The calculation revealed that no significant difference was observed among the tested lead shield positions. Nevertheless, the positioning of the lead shield between the X-ray tube and T2 was able to significantly reduce the scattered dose, up to 98%. Accordingly, the positioning of a lead shield is highly recommended, especially for exposure settings that lead to higher scatter values.

CONCLUSION

In this study, characterisation of the scatter dose distribution in the multi-bay resuscitation room has been performed. This characterisation is important due to the placement of multiple patient couches in the respective room. Hence, the amount of unnecessary, unintended exposure absorbed by patient and staff during the imaging procedure should be well estimated. The investigation was conducted using MCNP5 code. The assessment revealed that the highest scattered dose was calculated at T2. The main reason for this finding was due to the shorter distance between X-ray tube and T2. Yet, the calculated value was still lower than the dose limit for the public and radiation workers as recommended by the Basic Safety Standard regulations. The value was also lower than the daily background radiation dose of 8.22 μGy reported by NCRP Report No. 160. Nevertheless, it is strongly recommended that appropriate lead shielding should be considered when performing the imaging procedure at T1 while another patient is positioned at T2. In addition, although T3 and T4 received relatively small amounts of the scattered doses (much lower than the daily background radiation), the placement of protective lead shield should be considered. This is because the calculation only considered a single exposure setting. In a busy hospital, the number of imaging procedures performed daily is high. Hence, the cumulative dose to paramedic staff and patients may be very high.

ACKNOWLEDGEMENTS

This study was supported by the USM Short Term Grant (304/PPSK/6315167). The authors would like to thank the School of Health Sciences, USM and the Director of the Hospital Universiti Sains Malaysia (USM), Kubang Kerian, Kelantan for granting the permission to the investigators to use space and assets belonging to the hospital during the process of conducting the research. Special thanks goes to the staff of Hospital USM who had relentlessly assisted in making the research work successful.

REFERENCES

Archer, B. R., Fewell, T. R., Conway, B. J., & Quinn, P. W. (1994). Attenuation properties of diagnostic X-ray shielding materials. *Medical Physics, 21*, 1499-1507.

Catherine, M. H., John, H. M., Homer, C. T., & John, B. K. (2009). Radiation dose from initial trauma assessment and resuscitation: review of the literature. *Canadian Journal of Surgery, 52*(2), 147-152.

Chiang, H. W., Liu, Y. L., Chen, T. R., Chen, C. L., Chiang, H. J., & Chao, S. Y. (2015). Scattered radiation doses absorbed by technicians at different distances from X-ray exposure: Experiments on prosthesis. *Bio-Medical Materials and Engineering, 26*, S1641-S1650.

David, A. S., & Otha, W. L. (2009). National council on radiation protection and measurements report shows substantial medical exposure increase. *Radiology, 253*, 293-296.

Gu´erin, B., & Fakhri, G. E. (2008). Realistic PET Monte Carlo simulation with pixelated block detectors, light sharing, random coincidences and dead-time modeling. *IEEE Transactions on Nuclear Science, 55*(3), 942-952.

Goertz, L., Tsiamas, P., Karellas, A., Sajo, E., & Zygmanski, P. (2015). Monte Carlo simulation of a prototypical patient dosimetry system for fluoroscopic procedures. *Physics in Medicine and Biology, 60*(15), 5891-5909.

Hertrich, P. H. (2005). *Practical radiography: Principles and applications*. Erlangen, Germany: Publicis Corporate Publishing.

Lawrence, W. C. C., Chan, T. P., Ben, T. F. C., Kelvin, M., & Karl, K. L. F. (2015). Simulation, visualization and dosimetric validation of scatter radiation distribution under fluoroscopy settings. *Journal of Biomedical Engineering and Informatics, 1*(1), 93-102.

McVey, G., & Weatherburn, H. (2004). A study of scatter in diagnostic X-ray rooms. *The British Journal of Radiology, 77*, 28-38.

Owusu-Banahene, J., Darko, E. O., Charles, D. F., Maruf, A., Hanan, I., & Amoako, G. (2018). Scatter radiation dose assessment in the radiology department of cape coast teaching hospital-Ghana. *Open Journal of Radiology, 8*(4), 299-306.

Simpkin, D. J. (1989). Shielding requirements for constant potential diagnostic X-ray beams determined by a Monte Carlo calculation. *Health Physics, 56*, 151-164.

Simpkin, D. J. (1995). Transmission data for shielding diagnostic X-ray facilities. *Health Physics, 68*, 704-709.

Thomas, E. J., & Herman, C. (2009). *Introduction to health physics*. New York, NY: McGraw-Hill Medical.

Trinh, A. M., Schoenfeld, A. H., & Levin, T. L. (2010). Scatter radiation from chest radiographs: is there a risk to infants in a typical NICU? *Pediatric Radiology, 40*, 704-707.